Non-paraxial model for a parametric acoustic array

Milan Cervenka and Michal BednarikROC

Citation: The Journal of the Acoustical Society of America **134**, 933 (2013); doi: 10.1121/1.4813223
View online: http://dx.doi.org/10.1121/1.4813223
View Table of Contents: http://asa.scitation.org/toc/jas/134/2
Published by the Acoustical Society of America

Non-paraxial model for a parametric acoustic array

Milan Cervenka[a] and Michal Bednarik
Czech Technical University in Prague, Faculty of Electrical Engineering, Technicka 2, 166 27 Prague 6, Czech Republic

(Received 27 February 2012; revised 10 May 2013; accepted 24 June 2013)

This study is concerned with parametric radiation from an arbitrary axisymmetric planar source with a special focus on low-frequency difference-frequency fields. As a model equation accounting for nonlinearity, diffraction, and dissipation, the Westervelt equation is used. The difference-frequency-field patterns are calculated in the quasi-linear approximation by the method of successive approximations. A multi-layer integral for calculation of the acoustic field is reduced to a three-dimensional one by employing an approximate analytical description of the primary field with the use of a multi-Gaussian beam expansion. This integral is subsequently reduced in the paraxial approximation to a one-dimensional form which has previously been published in literature and which represents a means for fast calculations of secondary acoustic fields. The three-dimensional integral is calculated numerically and the numerical results predict nonzero amplitude of the low-frequency field in the vicinity of the source which is an effect that cannot be correctly encompassed in the paraxial approximation. © *2013 Acoustical Society of America*.
[http://dx.doi.org/10.1121/1.4813223]

PACS number(s): 43.25.Lj [ROC] Pages: 933–938

I. INTRODUCTION

Many contemporary acoustic applications make use of the fact that relatively directional low-frequency sound can be radiated from small sources by means of a parametric array.[1,2] This technique is based on radiation of two high-frequency sound beams (primary field) of similar frequencies $\omega_a \sim \omega_b$ in the same direction, where at least one of them must have a finite amplitude. As these waves propagate in medium, nonlinear interactions give rise to the generation of a secondary field consisting of higher harmonics, sum- and difference-frequencies, etc., by forming a phased array of virtual sources that resonantly pump acoustic energy into these components. It is obvious that a small percentage change of one of the primary frequencies results in a large percentage change in the difference-frequency, which means that wideband radiation (in difference-frequency) can be accomplished using a narrowband transducer.

Parametric radiation provides a means for generation of a substantially more directional and side-lobes-free sound beam at lower frequencies than is possible by direct small-signal radiation by a source of the same size. However, the former method is less efficient than the latter one.

Many papers have been dedicated to this topic. Far-field properties of the difference-frequency waves were studied in the pioneering work of Westervelt[1] based on the assumption that the nonlinear interactions are limited to the near-field of the primary waves which were modeled as collimated plane waves. Muir and Willette[3] calculated the sum- and difference-frequency field under the condition that the nonlinear interactions take place in the far-field of the primary waves, which were modeled analytically using the formula for the far-field of a uniformly vibrating piston. Garrett *et al.*[4] proposed a model for the parametric radiation from an arbitrary axisymmetric source in the quasilinear and parabolic approximation based on a numerical calculation of a triple integral. Kamakura *et al.*[5] studied the propagation of high-amplitude waves generated by a piston vibrating at two similar frequencies by numerical integration of the KZK equation using the algorithm proposed by Aanonsen *et al.*,[6] as well as experimentally. In Refs. 7 and 8, the authors utilized the method of multi-Gaussian beam (MGB) expansion of the sound field[9] for fast calculation of the secondary fields radiated by an arbitrary axisymmetric source in the quasilinear and paraxial approximation. The method was further extended for rectangular-aperture sources.[10,11]

The common characteristic of most of the above-mentioned papers and many others is the difference-frequency field calculated in the paraxial approximation. Even if this approach is applicable in the case of higher difference-frequencies as is undisputedly confirmed by many experiments, it is a question of whether the paraxial approximation provides correct results even in the case of lower difference-frequencies. This question is the subject of this paper. An analytic formula based on the three-fold integral is derived from the Westervelt equation; an appropriate algorithm is proposed for its numerical calculation. Certain numerical results are presented in order to demonstrate the differences between the low-frequency field patterns calculated using a fast algorithm based on the paraxial approximation and the proposed model which is not based on the paraxial approximation.

II. THEORY

A. Westervelt equation

The Westervelt wave equation[1,12] reads

[a]Author to whom correspondence should be addressed. Electronic mail: milan.cervenka@fel.cvut.cz

$$\Delta p' - \frac{1}{c_0^2}\frac{\partial^2 p'}{\partial t^2} + \frac{\delta}{c_0^4}\frac{\partial^3 p'}{\partial t^3} = -\frac{\beta}{\rho_0 c_0^4}\frac{\partial^2 p'^2}{\partial t^2}. \quad (1)$$

Here p' is the acoustic pressure, c_0 is small-signal sound speed, ρ_0 is ambient density of fluid, $\beta = (\gamma+1)/2$ is the coefficient of nonlinearity, where γ is the adiabatic exponent and

$$\delta = [\zeta + 4\eta/3 + \varkappa(1/c_V - 1/c_p)]/\rho_0$$

is the diffusivity of sound corresponding to thermoviscous attenuation, ζ and η stand for the bulk and shear viscosities, $\varkappa$ is the coefficient of heat conduction, and c_V and c_p are the specific heats at constant volume and pressure, respectively.

The method of successive approximations is used for integration of Eq. (1); its quasilinear solution is assumed to have the form

$$p' = p'_1 + p'_2,$$

where p'_1 is the linear solution (the first approximation) of Eq. (1) representing the primary field and p'_2 is a small correction to p'_1 (the second approximation, $|p'_2| \ll |p'_1|$) due to the nonlinear interaction representing the secondary field (second harmonics, sum- and difference-frequency waves, etc.).

As the acoustic field is assumed to be periodic in time, individual frequency components can be written in the form

$$p'_j(\boldsymbol{r},t) = p'_{0j}(\boldsymbol{r})\cos[\omega_j t - \phi_j(\boldsymbol{r})] = \frac{1}{2}[q_j(\boldsymbol{r})e^{-i\omega_j t} + q_j^*(\boldsymbol{r})e^{i\omega_j t}], \quad (2)$$

where $i = \sqrt{-1}$, $q_j(\boldsymbol{r}) = p'_{0j}(\boldsymbol{r})e^{i\phi_j(\boldsymbol{r})}$ is the complex amplitude of acoustic pressure and the asterisk denotes the complex conjugate (c.c.).

B. Primary field

For the two primary waves with angular frequencies ω_a and ω_b, where $\omega_a > \omega_b$, substitution of relation (2) into the linearized Eq. (1) yields

$$\Delta q_j + k_j'^2 q_j = 0, \quad (3)$$

where $j = a, b$ and $k'_j = \sqrt{k_j^2 + i\omega_j^3\delta/c_0^4} \approx k_j + i\alpha_j, k_j = \omega_j/c_0$ is the wavenumber and $\alpha_j = \omega_j^2\delta/2c_0^3$ is the thermoviscous attenuation coefficient at the frequency ω_j. In audio- and low ultrasonic-frequency region, relaxation processes are responsible for most of the sound absorption, which is in air dependent on temperature, atmospheric pressure, and water vapor content. The sound attenuation coefficient α_j for the given frequency ω_j can be generalized[13,14] to account for these effects.

Supposing that the vibrating piston radiating the primary wave is placed in a baffle at the plane $z = 0$ and the z-component of its vibration velocity reads $v_{zj}(x,y,t) = [w_j(x,y)e^{-i\omega_j t} + \text{c.c.}]/2$, then the solution of Eq. (3) can be constructed with Green's functions[15] in the form of the Rayleigh surface integral

$$q_j(\boldsymbol{r}) = -\frac{i\omega_j\rho_0}{2\pi}\int_{-\infty}^{\infty}\int_{-\infty}^{\infty} w_j(x'', y'')\frac{e^{ik'_j R_0}}{R_0}dx''dy'', \quad (4)$$

where $R_0 = |\boldsymbol{R}_0| = \sqrt{(x-x'')^2 + (y-y'')^2 + z^2}$ is the distance between a source element $dS'' = dx''dy''$ and the point, at which the acoustic field is calculated, see Fig. 1.

C. Difference-frequency secondary field

For the secondary difference-frequency wave with the angular frequency $\omega_d = \omega_a - \omega_b$, Eq. (1) reduces to

$$\Delta q_d + k_d'^2 q_d = \frac{\beta\omega_d^2}{\rho_0 c_0^4} q_a q_b^*. \quad (5)$$

As it is assumed that $(\partial q_d/\partial z)_{z=0} = 0$ (the plane $z = 0$ is assumed to be rigid and it does not vibrate at the angular frequency ω_d), the solution of Eq. (5) can be constructed with Green's functions[15] in the form of the volume integral

$$q_d(\boldsymbol{r}) = -\frac{\beta\omega_d^2}{4\pi\rho_0 c_0^4}\int_{z'=0}^{\infty}\int_{y'=-\infty}^{\infty}\int_{x'=-\infty}^{\infty} q_a(\boldsymbol{r}')q_b^*(\boldsymbol{r}') \times\left(\frac{e^{ik'_d R^+}}{R^+} + \frac{e^{ik'_d R^-}}{R^-}\right)dx'dy'dz', \quad (6)$$

where

$$R^- = |\boldsymbol{R}^-| = \sqrt{(x-x')^2 + (y-y')^2 + (z-z')^2},$$

$$R^+ = |\boldsymbol{R}^+| = \sqrt{(x-x')^2 + (y-y')^2 + (z+z')^2}$$

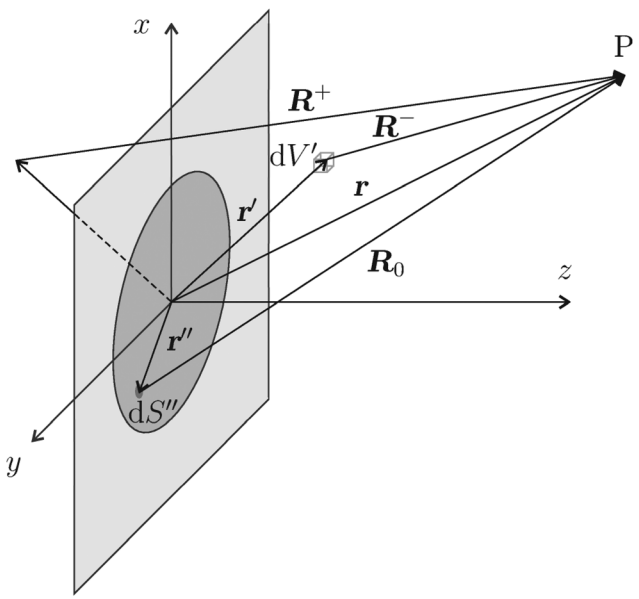

FIG. 1. Geometrical arrangement; P is the point, where acoustic field is determined.

(see Fig. 1). The Green's function used in this integral includes contribution of the element dV' of the virtual source formed by the primary field (the term containing R^-) as well as the contribution of its image representing the wave reflected from the plane $z = 0$ (the term containing R^+).

Equation (6) for calculation of $q_d(\boldsymbol{r})$ together with Eq. (4) represents the fifth-fold integral that is almost impossible to be calculated numerically. For this reason, an approximate analytic solution of integral (4) is used under the condition of the high-frequency primary field.

D. High-frequency approximation of the primary field

If the piston radiates at such frequencies that the condition $k_j a \gg 1$ is fulfilled, where a is the piston characteristic radius, the beam is reasonably directional; it is localized in the vicinity of the z axis and the waveforms are quasi-planar, the Green's function in Eq. (4) can be simplified into the paraxial (Fresnel) approximation[16] as

$$\frac{e^{ik'_j R_0}}{R_0} \approx \frac{1}{z}\exp\left\{ik'_j[z + [(x-x'')^2 + (y-y'')^2]/2z]\right\}. \quad (7)$$

If, subsequently, the distribution of the piston velocity is assumed to have an axial symmetry, it can be expanded into the series of the Gaussian functions[9]

$$w_j(x,y) \approx W_j \sum_{n=1}^{N} A_n e^{-B_n(x^2+y^2)/a^2},$$

where W_j represents amplitude and the complex coefficients A_n, B_n are calculated for an appropriate distribution by a numerical multidimensional optimization method.[9,17–19] Then, the integrals in Eq. (4) can be calculated analytically resulting in the formula

$$q_j(\boldsymbol{r}) = \rho_0 a^2 \omega_j W_j e^{ik'_j z} \sum_{n=1}^{N} \frac{A_n \exp\left[-\frac{k'_j B_n (x^2+y^2)}{k'_j a^2 + 2iB_n z}\right]}{k'_j a^2 + 2iB_n z}. \quad (8)$$

Substitution of this formula into Eq. (6) results in the three-fold integral for calculation of the difference-frequency wave

$$q_d(\boldsymbol{r}) = -\frac{\beta\rho_0 a^4 \omega_d^2 \omega_a \omega_b W_a W_b^*}{4\pi c_0^4 k'_a k'^*_b} \times \int_{z'=0}^{\infty} e^{i(k'_a - k'^*_b)z'} \sum_{n=1}^{N}\sum_{m=1}^{N} \frac{A_n A_m^* F_a F_b^*}{B_n B_m^*} \times \int_{r'=0}^{\infty} r' e^{-(F_a + F_b^*)r'^2} \times \int_{\varphi'=0}^{2\pi} \left(\frac{e^{ik'_d R^+}}{R^+} + \frac{e^{ik'_d R^-}}{R^-}\right) d\varphi' dr' dz', \quad (9)$$

where

$$F_a = \frac{k'_a B_n}{k'_a a^2 + 2iB_n z'}, \qquad F_b = \frac{k'_b B_m}{k'_b a^2 + 2iB_m z'}.$$

For the field at the symmetry axis, integral (9) reduces into the two-fold one

$$q_d(0,0,z) = -\frac{\beta\rho_0 a^4 \omega_d^2 \omega_a \omega_b W_a W_b^*}{2c_0^4 k'_a k'^*_b} \times \int_{z'=0}^{\infty} e^{i(k'_a - k'^*_b)z'} \sum_{n=1}^{N}\sum_{m=1}^{N} \frac{A_n A_m^* F_a F_b^*}{B_n B_m^*} \times \int_{r'=0}^{\infty} r' e^{-(F_a + F_b^*)r'^2} \left(\frac{e^{ik'_d R^+}}{R^+} + \frac{e^{ik'_d R^-}}{R^-}\right) dr' dz'. \quad (10)$$

Integrals (9) and (10) are calculated numerically.

E. Paraxial approximation of the secondary field

Using the paraxial approximation, integral (9) can be reduced to the form equivalent to the results presented formerly in the work.[8] The reduction consists of neglecting the term with R^+ in the Green's function (assuming that no secondary wave reflects from the source plane) and approximating the remaining term using a formula similar to Eq. (7). The integrals with respect to the coordinates x', y' can be then calculated analytically yielding

$$q_d(\boldsymbol{r}) = -\frac{i\beta\rho_0 a^4 \omega_d^2 \omega_a \omega_b W_a W_b^*}{2c_0^4 k'_a k'^*_b k'_d} \int_0^z e^{i(k'_a - k'^*_b)z'} \sum_{n=1}^{N}\sum_{m=1}^{N} \frac{A_n A_m^* F_a F_b^* \exp\{ik'_d|z-z'| - (F_a + F_b^*)(x^2+y^2)/[1 + i(F_a + F_b^*)F_g]\}}{B_n B_m^*[1 + i(F_a + F_b^*)F_g]} dz', \quad (11)$$

where $F_g = 2|z - z'|/k'_d$. The higher limit of integration is limited to z because in this approximation, it is assumed that only the nonlinear interactions between the source (piston) plane and the appropriate point contribute significantly to the sound field. This assumption is consistent with the paraxial approximation describing only one-way (forward) propagating secondary waves. The integral in Eq. (11) is calculated numerically.

III. NUMERICAL ALGORITHM

High-accuracy evaluation of multidimensional integrals is not easy because among other reasons it makes

great demands on computational performance. For this reason, it is necessary to utilize highly-efficient numerical algorithms.

In the case of integrals (9) and (10), the infinite computational domain was reduced to a reasonable size limited by a certain r_{max} and z_{max}. The repeated one-dimensional integration method[20] was used. Within this approach, the respective procedure calculating the inner integral is repeatedly invoked as required by the procedure calculating the outer integral.

In the case of the above-mentioned integrals, it is necessary to utilize algorithms allowing pre-defined accuracy of calculations (it was observed that with a fixed number of discrete points at which the integrated functions are evaluated, the accuracy of results decreases with the increasing difference-frequency value, because the integrated function becomes more oscillatory). Here, the Romberg method utilizing open formulas[20] was used for calculation of the individual one-dimensional integrals.

The numerical algorithms are implemented with use of the Numerical Recipes C++ library,[20] a substantial reduction of the computational time was achieved by parallelization of the algorithms using the OpenMP library and running on a multi-processor computer.

Coefficients of the MGB decomposition of the piston velocity distribution were calculated using a heuristic optimization method.[19]

IV. RESULTS

Within the numerical calculations, it was assumed that the source velocity distribution possesses the form

$$v_z(r,t) = \mathrm{e}^{-(r/a)^{16}}[v_{0a}\cos(2\pi f_a t) + v_{0b}\cos(2\pi f_b t)], \quad (12)$$

which means that the two-frequency vibration is almost spatially uniform within the circle of radius a; here $a = 0.2$ m. The corresponding coefficients of the MGB decomposition are listed in Table I. In all the presented cases $f_a = 50$ kHz and $f_b = f_a - f_d$, where f_d is required difference-frequency. The acoustic field is assumed to be radiated into the air with the temperature of 24 °C, atmospheric pressure 101 325 Pa, and 40% relative humidity. A model accounting for molecular relaxation processes[13] was used for calculation of the sound absorption coefficients α_j.

TABLE I. Complex coefficients of decomposition of the spatial part of function (12) into the series of Gaussian functions.

n	A_n	B_n
1	1.952546 − 7.094992i	5.627804 − 10.20442i
2	−9.479406 + 5.913680i	5.036574 + 4.307618i
3	7.678386 + 0.949987i	4.017862 + 0.175230i
4	5.963587 − 5.346673i	4.396490 + 5.519961i
5	−7.478762 − 0.945619i	4.348546 − 3.827380i
6	−3.949745 + 1.589160i	4.008304 − 10.03536i
7	−0.224418 + 0.091363i	1.951061 + 9.945993i
8	6.537564 + 4.840994i	7.537466 − 7.511751i

As in this case $k_a a = 192 \gg 1$, the primary wave is well-directional and the paraxial approximation for calculation of the primary field is applicable.

Figure 2 shows the distribution of acoustic pressure amplitude at the frequency f_a along the axis of symmetry calculated in the linear approximation using Eq. (8) (paraxial approximation) and using the Rayleigh integral (4). It can be observed that except for the close vicinity of the source, the results are almost identical so that the paraxial approximation of the formulas for calculation of the primary field does not decrease the accuracy of the algorithm in a substantial way.

The distribution of normalized acoustic pressure amplitude at difference frequency f_d along the piston axis calculated in the non-paraxial approximation using Eq. (10) and in the paraxial approximation using Eq. (11) is shown in Fig. 3. For individual frequencies f_d, the normalized acoustic pressure amplitude is defined as the ratio of the acoustic pressure amplitude and the maximum acoustic pressure amplitude calculated in the paraxial approximation.

For all the difference frequencies f_d, the paraxial equation (11) predicts a zero difference-frequency field at the piston and a steep increase of its amplitude with increasing distance from the piston, which becomes steeper as the difference frequency lowers. By contrast, the non-paraxial Eq. (10) predicts a non-zero amplitude of the acoustic field for very low difference-frequencies. This situation is caused by the fact that for low f_d, the product $k_d L$, where L is the effective length of the phased virtual source, attains a small value which means that the source is not highly directional. It radiates partly in the direction opposite the primary waves and this backwards-traveling wave reflects from the source plane.

For higher values of the difference-frequencies (in this case for $f_d = 2000$ Hz), both the equations provide almost the same results. This is caused by a higher value of $k_d L$ resulting in a higher directivity of the virtual source and negligible backward radiation The differences between the results for all the frequencies f_d decreases with the distance from the piston.

Figure 4 shows a comparison of the directivity of the difference-frequency wave in the far-field (at the distance of $200a$ from the piston) calculated using the non-paraxial model (9) and in the paraxial approximation using the

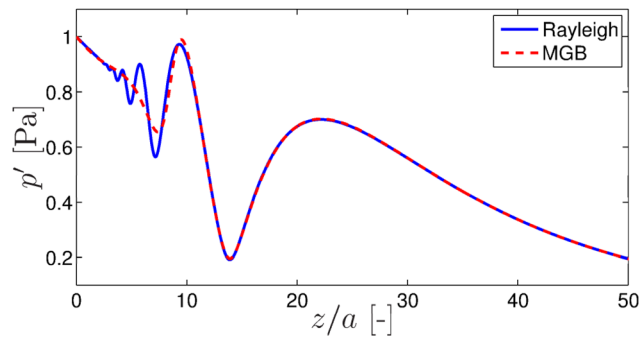

FIG. 2. (Color online) Distribution of the primary wave acoustic pressure amplitude along the piston axis calculated using Eq. (8) and the Rayleigh integral (4), $f_a = 50$ kHz, $v_{0a} = 2.43 \times 10^{-3}$ m · s^{-1}.

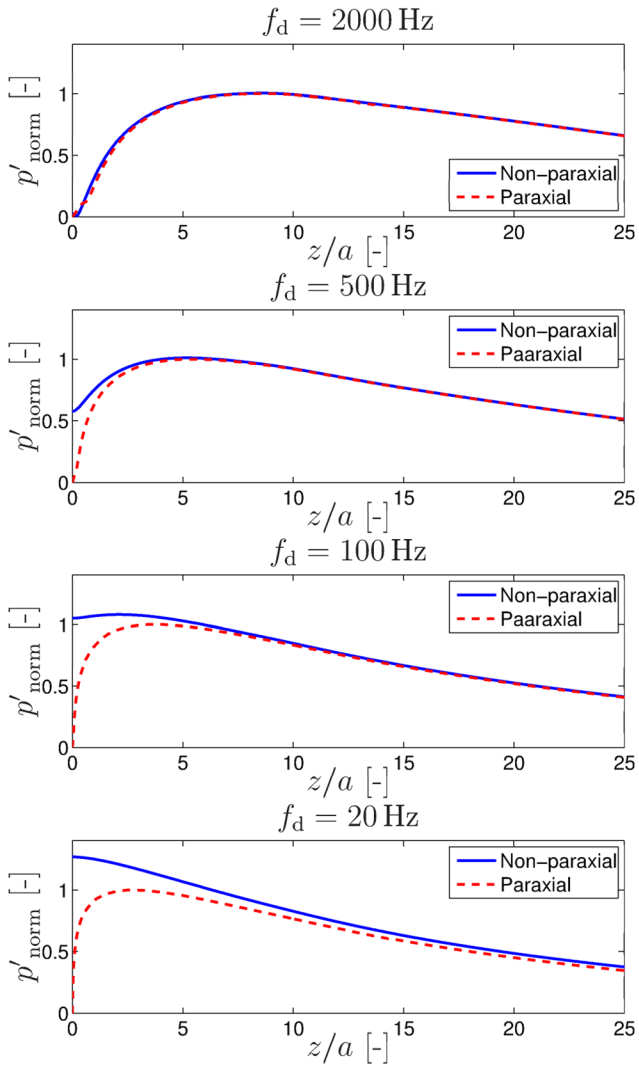

FIG. 3. (Color online) Distribution of normalized acoustic pressure amplitude of the difference-frequency wave along the piston axis for different values of f_d. In the non-paraxial approximation, integral (10) was used, in the paraxial approximation, integral (11) was used.

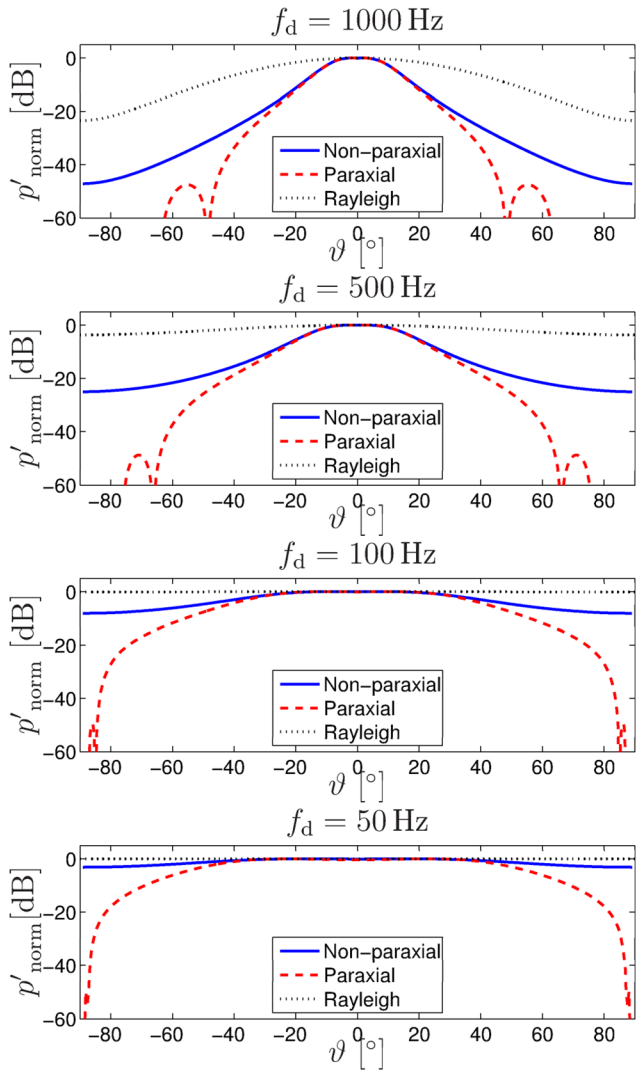

FIG. 4. (Color online) Comparison of the difference-frequency wave directivity calculated in the paraxial and non-paraxial approximation. For illustration, directivity of the wave radiated directly at the frequency f_d is shown (calculated using the Rayleigh integral). ϑ is the polar angle (with respect to the symmetry axis).

integral (11). The case of the direct radiation of a small-amplitude wave with frequency f_d, calculated using the Rayleigh integral (4) is also included. All the courses are normalized to have 0 dB at the axis of symmetry (in all the presented cases, the difference-frequency acoustic field predicted by the paraxial and non-paraxial models are the same at the axis of symmetry, $\vartheta = 0°$).

It can be observed that even for very low frequencies, up to the angle ca. 30°, both the approximations (paraxial and non-paraxial) provide the same results. For bigger angles, the paraxial approximation predicts a lower amplitude of the acoustic field than the approximation that is non-paraxial. It can be observed that directivity of the difference-frequency wave (calculated using the non-paraxial approximation) decreases with its frequency. For instance, at the angle of $\vartheta = 45°$ with respect to the axis, the acoustic pressure amplitude decreases by 28.8 dB at 1000 Hz, by 17.4 dB at 500 Hz, by 3.9 dB at 100 Hz, and only by 0.9 dB at 50 Hz. At this frequency, the acoustic field is almost omnidirectional.

V. CONCLUSION

A formula based on a three-fold integral was proposed for calculation of the difference-frequency wave caused by nonlinear interactions of the two-frequency primary wave generated by a baffled axisymmetric piston. As the formula is not based on the paraxial approximation of the secondary field, it can be used for calculation of near-field as well as wide-angle far-field patterns. On the other hand, the numerical calculation of multi-fold integrals requires a relatively large amount of the computational work compared with the fast algorithms based on the paraxial approximation and one-fold integration. Nevertheless, the proposed formula allows a direct comparison of the numerical results with the ones obtained in the paraxial approximation under otherwise the same conditions and thus it allows delimitation of the applicability of the paraxial model.

The numerical results clearly demonstrate that in the case of the low-frequency secondary field, its amplitude is

nonzero at the vicinity of the source, which is caused by low directivity of the virtual source and which is a result that cannot be predicted by any model based on the one-way (forward) propagation of acoustic waves.

ACKNOWLEDGMENTS

This work was supported by GACR Grant No. P101/12/1925. The numerical calculations were performed on a SGI Altix XE 340 computer at the Computing and Information Centre of CTU.

[1]P. J. Westervelt, "Parametric acoustic array," J. Acoust. Soc. Am. **35**, 535–537 (1963).
[2]M. F. Hamilton, "Sound beams," in *Nonlinear Acoustics*, edited by M. F. Hamilton and D. T. Blackstock (Academic Press, San Diego, CA, 1998), Chap. 8, pp. 246–250.
[3]T. G. Muir and J. G. Willette, "Parametric acoustic transmitting arrays," J. Acoust. Soc. Am. **52**, 1481–1486 (1972).
[4]G. S. Garrett, J. Naze Tjøta, and S. Tjøta, "Near-field of a large acoustic transducer, Part II: Parametric radiation," J. Acoust. Soc. Am. **74**, 1013–1020 (1983).
[5]T. Kamakura, N. Hamada, K. Aoki, and Y. Kumamoto, "Nonlinearly generated spectral components in the near-field of a directive sound source," J. Acoust. Soc. Am. **85**, 2331–2337 (1989).
[6]S. I. Aanonsen, T. Barkve, J. Naze Tjøta, and S. Tjøta, "Distortion and harmonic generation in the near-field of a finite amplitude sound beam," J. Acoust. Soc. Am. **75**, 749–768 (1984).
[7]D. Ding, Y. Shui, J. Lin, and D. Zhang, "A simple calculation approach for the second harmonic sound field generated by an arbitrary axial-symmetric source," J. Acoust. Soc. Am. **100**, 727–733 (1996).
[8]D. Ding, "A simplified algorithm for the second-order sound fields," J. Acoust. Soc. Am. **108**, 2759–2764 (2000).
[9]J. J. Wen and M. A. Breazeale, "A diffraction beam field expressed as the superposition of Gaussian beams," J. Acoust. Soc. Am. **83**, 1752–1756 (1988).
[10]K. Sha, J. Yang, and W. S. Gan, "A complex virtual source approach for calculating the diffraction beam field generated by a rectangular planar source," IEEE Trans. Ultrason. Ferroelectr. Freq. Control. **50**, 890–897 (2003).
[11]J. Yang, K. Sha, W. S. Gan, and J. Tian, "Nonlinear wave propagation for a parametric loudspeaker," IEICE Trans. Fundamentals **E87-A**, 2395–2400 (2004).
[12]M. F. Hamilton and C. L. Morfey, "Model equations," in *Nonlinear Acoustics*, edited by M. F. Hamilton and D. T. Blackstock (Academic Press, San Diego, CA, 1998), Chap. 3, pp. 54–56.
[13]H. E. Bass, L. C. Sutherland, A. J. Zuckerwar, D. T. Blackstock, and D. M. Hester, "Atmospheric absorption of sound: Further developments," J. Acoust. Soc. Am. **97**, 680–683 (1995).
[14]H. E. Bass, L. C. Sutherland, A. J. Zuckerwar, D. T. Blackstock, and D. M. Hester, "Erratum: Atmospheric absorption of sound: Further developments [J. Acoust. Soc. Am. **97**, 680–683 (1995)]," J. Acoust. Soc. Am. **99**, 1259 (1996).
[15]P. M. Morse and K. Uno Ingard, *Theoretical Acoustics* (McGraw-Hill, New York, 1968), Chap. 7.
[16]J. W. Goodman, *Introduction to Fourier Optics* (McGraw-Hill, New York, 1996), Chap. 4, pp. 66–73.
[17]H.-J. Kim, L. W. Schmerr, and A. Sedov, "Generation of the basis sets for multi-Gaussian ultrasonic beam models: An overview," J. Acoust. Soc. Am. **119**, 1971–1978 (2006).
[18]D. Ding and Y. Zhang, "Notes on the Gaussian beam expansion," J. Acoust. Soc. Am. **116**, 1401–1405 (2004).
[19]M. Cervenka, M. Bednarik and P. Konicek, "Numerical simulation of parametric field patterns of ultrasonic transducer arrays," on the CD-ROM: *2009 EEE International Ultrasonics Symposium Proceedings*, September 20–23, 2009, Roma (available also at http://ieeexplore.ieee.org/, DOI: 10.1109/ULTSYM. 2009.5441905; last viewed May 23, 2013).
[20]W. H. Press, S. A. Teukolsky, W. T. Vetterling, and B. P. Flannery, *Numerical Recipes 3rd Edition: The Art of Scientific Computing* (Cambridge University Press, Cambridge, 2007), Chap. 4.